Multiscale Modeling of Muscular-Skeletal Systems

Gang Seob Jung and Markus J. Buehler

Laboratory for Atomistic and Molecular Mechanics, Department of Civil and Environmental
Engineering, Massachusetts Institute of Technology, Cambridge, Massachusetts 02139;
email: mbuehler@MIT.edu

Keywords

muscular-skeletal systems, multiscale modeling, elastin, collagen, hydroxyapatite, 3D printing design

Abstract

Multiscale modeling of muscular-skeletal systems—the materials and structures that help organisms support themselves and move—is a rapidly growing field of study that has contributed key elements to the understanding of these systems, especially from a multiscale perspective. The systems, including materials such as bone and muscle, have hierarchical structures ranging from the nano- to the macroscale, and it is difficult to understand their macroscopic behaviors, both physiological and pathological, without knowledge of their hierarchical structures and properties. In this review, we discuss the methods of multiscale modeling. Through a series of case studies about key materials in muscular-skeletal systems, we describe how different methods can bridge the gap between hierarchical structures and their roles in the systems' mechanical properties. In particular, we emphasize the importance of the quality of minerals in bone. Finally, we discuss biomimetic material designs facilitated by additive manufacturing technology.

Contents

1. INTRODUCTION

Muscular-skeletal systems are composed of bones, muscles, tendons, ligaments, cartilages, and other connective tissues. The most fundamental and crucial functions of these systems are to protect vital organs, support body structures, and facilitate organism mobility (1). Whereas the skeletal and smooth muscles of the muscular system allow movement of the body, the skeletal system consists of bones and joints, which provide the shape and form of the body, protect soft organs, store vital minerals, and produce blood (2). Within the skeletal system, tendons and ligaments are flexible and tough bands of fibrous connective tissues. Tendons mainly connect bones to muscles, whereas ligaments connect bones to bones (3, 4). Cartilage bridges the joints between bones, providing lubrication and preventing wear (5). All these systems largely consist of similar materials: collagen, mineral, and elastin. It is amazing that diverse and multiple functions and properties can be derived from this set of three materials (4, 6). In this review, we discuss these three materials and how their properties can be described with multiscale modeling. The purpose of this article is to provide a comprehensive and integrated point of view of the basic model methods with applications from the atomistic to the continuum scale, as well as to assess the interactions between the building blocks that result in complex material functions.

We experience multiscale dynamics of the muscular-skeletal systems every day even without explicitly recognizing it. For example, bone fractures and injuries from an accident result from nanoscale bond breaking in a relatively short time, whereas healing and remodeling of bones facilitated by cellular mechanisms take more than weeks of growth and rearrangement (6, 7). Two

challenging features of these systems need to be addressed in order to build proper models that accurately describe their behaviors. First, parts of the systems have complex hierarchical structures at different length scales that lead to different deformation or failure responses under external loadings (8–10). Second, the materials of the systems are heterogeneous mainly because of the continuous localized rehabilitation and growth in the systems (11–14). In particular, ordered and disordered phases of bone at different scales are revealed with three-dimensional (3D) structural analysis (15). Although hierarchies and heterogeneities complicate the process of building models of the systems, they are responsible for enhancing the systems' performance with lower mass and relatively less costly materials compared with conventional engineering materials (16–18).

Figure 1 illustrates the hierarchical structures of various materials that make up the muscular-skeletal systems from the nano- to the macroscale (6, 19–21). The elastin fiber is one of the main components of various connective tissues; it is composed of tropoelastins and microfibrillar arrays with cross-links (19). The basic building blocks of tendons and muscles are tropocollagen molecules. These molecules form fibers, and the fibers further constitute hierarchical bundles of fibers, which ultimately assemble into tendons and muscles. The fundamental building blocks of bone are carbonated hydroxyapatite (HAP) minerals and tropocollagen molecules, which form mineralized collagen fibrils and fibers (22, 23). Radially oriented fibers form approximately cylindrical osteon structures, and bundles of osteons with blood vessels and nerves make up bone (8).

These hierarchical structures show different deformation and failure behaviors. For example, the deformation of collagen fibrils is sliding, but the deformation of osteons accompanies generations of microcracks. Due to these hierarchical structures, deformation and failure of the systems cannot be described simply by one conventional method. Instead, the behaviors of the systems can be understood by considering various deformation and failure mechanisms at different length and timescales (8, 24). Moreover, conventional approaches with computer simulations can handle only specific ranges of time and length because disparate laws and methods of modeling govern different scales. For instance, the properties of water can be studied at different scales (**Supplemental Figure 1**). The physical scale of a river is on the order of kilometers, and the flow of the river is governed by Navier–Stokes equations (25). A cup of water is orders of magnitude smaller, and splashes of water can be modeled by smoothed particle hydrodynamics (26). The phase transition from water to ice is related to the change of the hydrogen-bond (H-bond) network at the nanoscale, which can be captured by molecular dynamics (MD) (27). The phenomenon of proton transfers between water molecules is related to covalent bond breaking and reforming; reactive MD simulation can capture the changing covalent bonds (28). Finally, all electrons in a water molecule are governed by the Schrödinger equations. The above examples are separable problems that can be solved at one specific length and timescale. However, problems such as the breaking of a huge iceberg are governed by multiscale dynamics. As the iceberg breaks, the initiation and propagation of failure are generally complex and difficult to solve with conventional continuum methods. Multiscale modeling is a new paradigm that focuses on integrating and connecting scale-disparate theories and computational methods with appropriate approximations and profound insights (24).

In addition to the complications that arise from multiscale dynamics, atomistic factors, such as mineral phases of bone or mutations of collagens, significantly affect the mechanical properties of the muscular-skeletal systems. Due to their nanoscale characteristics and difficulties in isolating components, experimental approaches are extremely limited; thus, building higher-scale models with parameters derived from experiments is formidable. Lower-scale models also have limitations in terms of accessible sizes and times, making phase transitions such as mineralization and self-assemblies of proteins very challenging. Multiscale modeling bridges these different scales by simplifying lower-scale models as several parameters for higher-scale models. The advent of
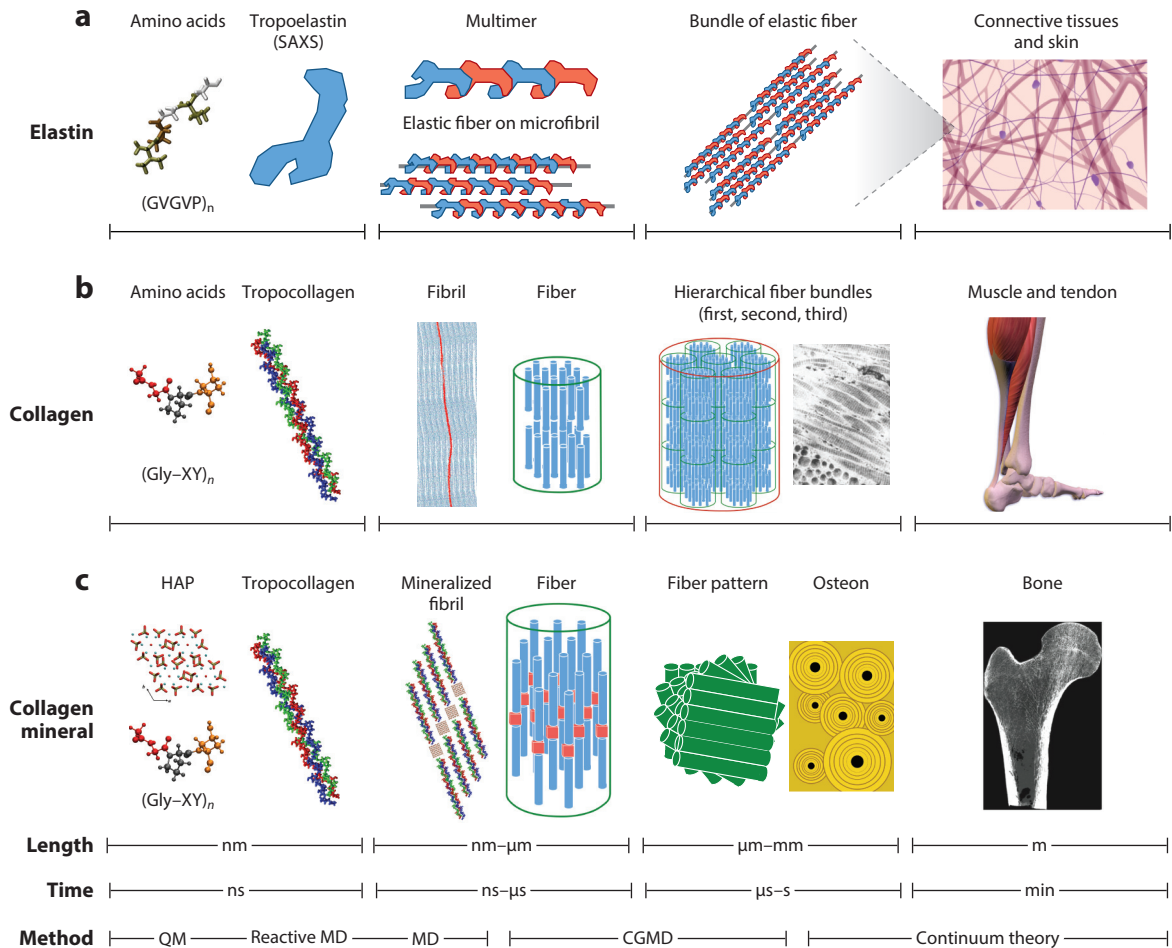
Supplemental Material

Figure 1

The hierarchical structures of various materials of muscular-skeletal systems: elastin, collagen, and minerals with different length scales, timescales, and multiscale methods. (*a*) The basic building block of elastic fibers is the amino acid sequence GVGVP, which forms tropoelastin. Tropoelastin molecules are deposited on a bundle of microfibrils with cross-links, constructing elastin fibers. (*b*) The basic building block of tendons and muscles is a tropocollagen molecule with a helix structure. Assemblies of tropocollagen molecules build fibrils, fibers, and their bundles. (*c*) The basic building blocks of bone are hydroxyapatite (HAP) minerals and tropocollagen molecules, constructing mineralized collagen fibrils. Osteon structures are composed of fiber patterns of the mineralized collagen fibrils. Abbreviations: CGMD, coarse-grained molecular dynamics; MD, molecular dynamics; QM, quantum mechanics; SAXS, small-angle X-ray scattering. Image of collagen fibers modified with permission from Reference 107. Copyright 1977, Wiley. Image of connective tissue modified from Reference 108, licensed under CC BY-SA 4.0. Image of bone model modified with permission from Reference 109. Image of tendon adapted from Wikimedia Commons (**https://commons.wikimedia.org/wiki/File:Achilles_Tendon_Tear. png**), licensed under CC BY-SA 4.0.

parallel computing technology accelerates the development of multiscale modeling to deal with more degrees of freedom. It enables the handling of more particles or elements in the system to obtain more statistically accurate values to represent the properties of the systems. Properties determined from a lower scale, such as a diffusion coefficient and mechanical properties, can be used as input for a higher-scale model. This bottom-up approach to studying materials is very

attractive due to quantum mechanics (QM). Although QM can deal only with a small number of atoms or pristine systems, it can predict the properties of materials without parameters derived from experiments but on the basis of fundamental theory rooted in chemistry and physics (29). Thus, simulation-based design concepts can be tested, saving tremendous cost and time in developing engineering and biomedical materials (30).

The most critical part of multiscale modeling is deciding which properties play significant roles in the higher level of the system (31, 32). This is not a typical problem, and it requires rigorous validation of the mechanism found. Current additive manufacturing technology, such as 3D printing, is a valuable tool to examine or validate new understanding from multiscale modeling by allowing the construction of complex geometries in combination with various materials (33). Thus, we can test simplified systems to examine the mechanisms, and the results can be utilized to establish a design rule for novel materials (34, 35).

2. MULTISCALE MODELING

Many computational methods have been developed to study the properties of materials at different discrete length and timescales, such as QM, MD, coarse-grained molecular dynamics (CGMD), and the finite element method (FEM). We address the basic concepts of each method currently employed in multiscale modeling. Also, we discuss advanced MD techniques to overcome a well-known limitation of atomistic modeling (36).

2.1. Quantum Simulation

The most fundamental scale within the multiscale paradigm is the atomistic scale. Components of the muscular-skeletal system are continuously growing and are occasionally damaged. Both growth and failure initiate from the atomistic scale through chemical bonds forming and breaking (24). The interactions between atoms are governed by the distribution and states of their electrons. Quantum simulations allow us to predict the behavior of electrons and understand their corresponding properties, such as light absorptions, band structures, and electromagnetic characteristics. In principle, for a given geometry of atoms, quantum simulation does not require experimentally fitted parameters (37). Thus, we can model the system with a bottom-up approach and develop modeling-driven material designs.

Electrons have discrete energy values based on their quantum states, and their behavior can be derived from the Schrödinger equations. However, solving the equations for all electrons even in small systems is almost impossible. Approximations simplifying the many-body interactions of electrons to noninteracting electrons in an effective potential are employed in density functional theory (DFT) (38, 39). DFT enables handling more atoms in systems and has been successfully applied to solid-state physics (40). However, DFT is not sufficiently accurate to deal with transition states or van der Waals (VdW) interactions. Ab initio quantum chemistry calculation, based on the Hartree–Fock (HF) method, is another approach to deal with electrons. Many extensions of the HF method have been proposed for better accuracy (41). However, the computational cost increases significantly as the accuracy increases; therefore, the method should be chosen carefully according to the properties to be studied. At present, the use of quantum simulations in multiscale modeling is limited to mechanical properties and structures of materials at the ground state, which are well described by either DFT or ab initio calculations. The properties and structures derived from quantum simulations can be utilized to determine the unknown input parameters in MD for materials in the muscular-skeletal system (42). In this review, we describe the use of DFT calculations to study the mechanical properties of the minerals in bone.

2.2. Classical Molecular Dynamics

Because the number of atoms a quantum simulation can handle is extremely limited, further simplifications are necessary to deal with a greater number of atoms. Classical MD is a way to deal with atoms or molecules on the basis of their interactions, in which the electronic structures of the atoms are not changed. Instead, force fields or potentials are adopted for the effects of electron states. After Alder & Wainwright (43) performed the first MD simulation with hard spheres in the late 1950s, various potential forms have been developed and used in MD simulations. The most fundamental potential that includes repulsive and attractive terms is the Lennard-Jones (LJ) potential, commonly expressed as

$$V_{LJ}(r) = 4\varepsilon \left[\left(\frac{\sigma}{r} \right)^{12} - \left(\frac{\sigma}{r} \right)^{6} \right], \tag{1}$$

where ε is the depth of the potential, σ is the distance where the potential value is zero, and r is the distance between particles. The LJ potential has had great success in describing the behavior of noble gases such as argon (44). This potential is widely used in describing VdW interactions in various systems. For biomolecules such as lipids and protein systems, an empirical force field known as CHARMM has been proposed (45). The basic form of the force field is

$$V_{system} = V_{bond} + V_{angle} + V_{dihedral} + V_{improper} + V_{VdW} + V_{Coulomb}. \tag{2}$$

Other force fields such as AMBER (46) and GROMOS (47), developed on the basis of different experimental data or ab initio calculations, have also been proposed with similar constituent terms to describe biomolecules. The force fields usually have terms for torsion, bond stretching, angle, and nonbonded interactions (**Supplemental Figure 2**), and the parameters have been improved over time for better descriptions of properties from experiments, such as secondary structures (48).

From these force fields, the Hamiltonian of a system is defined as $H(p_i, q_i) = K(p_i) + E(q_i)$, where K is the kinetic energy term, E is the potential energy term described by the force fields, and p_i and q_i are the momentum and position of the ith particle, respectively. From this Hamiltonian the time derivatives of position and momentum can be derived, and the trajectories of the atoms can be obtained by numerical integration (49). The system is described as a microcanonical ensemble representing all possible states of a mechanical system having the same total energy. Because the controllable macroscopic variables are the number of particles (N), total volume (V), and energy (E), the microcanonical ensemble is also termed the NVE ensemble. However, NVT (canonical) and NPT (isobaric–isothermal) ensembles are generally adopted in MD simulations because temperature (T) or pressure (P) is usually utilized as a macroscopic variable in experiments (50–52).

A proper time step should be chosen for the conservation of the total Hamiltonian to ensure the appropriate sampling of the correct ensemble. In biomolecular systems, a time step of 1 fs is sufficient for unconstrained atomistic systems, whereas a longer time step of 2 fs can be utilized together with H-bond constraints (53). Short integration time steps prevent attaining simulation timescales beyond microseconds in MD simulations. This would require more than a billion steps, a significant task even for modern supercomputers. In this review, we demonstrate how MD simulations can be utilized to model the deformation of collagen molecules, minerals, and their interactions at the nanoscale.

2.3. Reactive Force-Field Molecular Dynamics

The deformation and mechanical responses of biomolecules are governed mainly by changes in H-bond networks (54). However, the breaking of covalent bonds is also critical to understanding the mechanisms of protein unfolding and failure (24, 55). Nonreactive force fields such as

CHARMM are capable only of describing atoms near their ground states because these force fields ignore quantum chemical states as an approximation. In contrast, reactive force fields can capture the changes in bonding by considering bond orders that are estimated from the relative distances and angles between particles. The bond orders enable one to approximate the quantum chemical states of particles for the formation or breakage of bonds in the systems (**Supplemental Figure 2**) (56). Although reactive force fields capture the change of quantum states and are less computationally expensive than quantum simulations, the number of atoms in the system is still limited to tens of thousands, which is much less than in classical MD simulations (more than billions) (28). Thus, a hybrid concept can be utilized for efficiency that uses the reactive force field only for highly reactive parts of the system (57). In this review, we show how the reactive force field is used to parameterize unknown parameters of cross-links in collagen fibrils for CGMD.

2.4. Coarse-Grained Molecular Dynamics

Due to the temporal and spatial limitations of MD simulations, other approaches are required to deal with mesoscopic-scale (micrometer-scale) models. CGMD follows the simple classical MD scheme and deals with groups of atoms as simplified beads. The interactions between these beads are defined mainly by LJ potentials and harmonic springs. Because the addressable timescale arises from how many atoms a bead represents, we can choose various timescales by controlling the coarse-graining level and the parameters for interactions. Thus, the methods used to systematically derive the parameters and tune them under reasonable assumptions are important for obtaining reliable results. One of the methods used to systematically derive the parameters for biomolecules is the MARTINI force field (58), which is based on the partitioning of free energy and mapping of atomic positions to coarse-grained beads. The basic rule of the MARTINI force field is that four heavy atoms are approximated as a single coarse-grained bead with a single interaction center. The force field performs well in modeling protein structures and aggregations of simple peptides (59). However, replacing four atoms with one bead does not significantly reduce the computational restrictions on systems' sizes. In this review, we discuss the deformation and failure of collagen fibrils and mineralized collagen fibrils with coarser beads than those used in the MARTINI force field.

2.5. Continuum Theory

The continuum approach is the most common method to describe systems at the macroscale, and this is a very successful way to describe the many structural problems of homogeneous materials. In this approach, a system is modeled as a continuous material rather than being composed of particles, without explicitly accounting for a material's internal structure. One of the basic models in continuum mechanics is based on Hook's relation, in which the elongation of elements is proportional to the applied external force. When a force F is applied to a beam of length L and cross-sectional area A, the extension is given as Δu (**Supplemental Figure 3**). The equation $F = k\Delta u$ can be normalized by the unit volume ($V = AL$) as

$$\sigma = \frac{F}{A} = \frac{Lk}{A}\frac{\Delta u}{L} = E\varepsilon, \tag{3}$$

where σ, E, and ε are defined as stress, Young's modulus, and strain, respectively. This linear relation between stress and strain governs the behavior of brittle materials in the elastic regime, where the deformation is reversible. However, the deformation of materials such as metals generally has a plastic deformation regime in which irreversible deformation occurs.

Griffith (60) and Irwin (61) developed linear elastic fracture mechanics (LEFM). The Griffith criterion states that failure of materials with a flaw occurs when the stored strain energy is large

enough to create two new surfaces under uniaxial loading. The energy release rate G, which represents the dissipation of stored strain energy per unit of newly created surface area during the crack propagation, is defined by

$$G = \frac{\partial U}{\partial A},\qquad(4)$$

where U is the stored strain energy available for crack propagation and A is surface area. A small crack can propagate when $G = 2\gamma$, where γ is surface energy (the energy necessary to create a new surface; two new surfaces are created as the crack advances). The failure strength of a linear system with a small crack is given by $\sigma_c = \sqrt{(EG)/(\pi a)}$, where E and a are Young's modulus and length of the crack, respectively. LEFM can describe the failure of brittle and homogeneous materials such as glass (60).

In multiscale modeling, Young's modulus and the energy release rate can be readily obtained from atomistic simulation by calculating the corresponding materials' elastic constants and surface energy. However, the energy release rate is not simply 2γ when the dissipated energy constitutes a large portion of the energy release rate, such as in heterogeneous materials. A better expression under this situation would be $G = 2\gamma + G_{\text{diss}}$. The energy release rate of inhomogeneous materials can be obtained from atomistic simulations by measuring the total external work for failure of the systems (62).

The deformations and damages of the muscular-skeletal system are locally inhomogeneous, which is challenging to describe with LEFM. The cohesive zone model has been widely adopted for describing damages on the basis of the critical energy release rate. Each element can take damage according to its local stress and history of damages (**Supplemental Figure 3**). The basic elastic properties and the energy release rate are key to connecting particle-based simulations (QM, MD, and CGMD) to continuum theory (FEM). However, a more systematic framework needs to be developed to bridge these disparate methods.

2.6. Replica Exchange Molecular Dynamics

When the system size increases, more computing units can help reduce computational time by domain decomposition (63, 64). However, it is challenging to accelerate a simulation in the time domain because the time evolution of the system depends on the previous steps or states. On one hand, this dependency limits particle simulations, including MD and CGMD, to their conventional timescale on the order of nanoseconds or, at most, hundreds of nanoseconds. Protein folding occurs on the timescale of microseconds to milliseconds, which puts the folding of most large proteins out of reach of conventional MD. On the other hand, this limitation comes from the complex energy landscape of systems: Short simulations cannot overcome barriers/local minima to sample other configurations effectively. Although the time domain cannot be parallelized, the problem of being trapped in local minima can be alleviated in other ways. Sugita & Okamoto (36) have proposed replica exchange molecular dynamics (REMD), which utilizes multiple replicas with slightly different temperatures to overcome the barriers but produce correct ensembles (**Supplemental Figure 4**). This method enables systems to overcome complex energy landscapes and reach the global minimum much faster than conventional MD. In this review, we discuss how REMD is utilized for unknown structures of a part of a tropoelastin molecule.

3. MULTISCALE MODELING OF ELASTIN AND COLLAGEN

An important class of biomolecules in muscular-skeletal systems consists of proteins. Proteins are large molecules responsible for various biological functions, such as molecular transport, DNA replication, metabolic reactions, and enzymatic reactions (65). Each molecule is made of one

or more polypeptide chains of various types of amino acids, which are the fundamental building blocks of proteins. The sequences of amino acids are determined by the sequence of the corresponding gene that codes for this particular protein. The series of amino acids determines how the chains fold into complex structures and the biological functions of the protein. In this section, we review multiscale modeling of collagen and elastin: the most abundant and important proteins for mechanical properties in the muscular-skeletal systems.

3.1. Molecular Dynamics of Elastin

Elastin is a highly flexible and largely deformable biomaterial found in various parts of the muscular-skeletal systems, such as tendons, ligaments, and cartilages. Elastin is usually found in the form of fibers in the extracellular matrix of connective tissues, composed of microfibrils and amorphous tropoelastin molecules (18). Although only one gene produces tropoelastin, alternative splicing enables the formation of diverse tropoelastin isoforms. These splice variants can fulfill the various functional and structural requirements of the fibers in various tissues (66).

It remains challenging to determine a fully atomistic structure of tropoelastin from experiments, as it does not form a crystal structure. Also, insolubility and complex cross-link networks present significant difficulties in isolating this molecule. There are 34 exons in the human tropoelastin transcript, where exclusion of domain 22 in wild-type (WT) tropoelastin is believed to be critical for forming a flexible hinge region for elastic fiber assembly (**Figure 2a**) (67). Yeo et al. (68) have studied the effect of the hinge region on the dynamics and structures of tropoelastin with small-angle X-ray scattering (SAXS) and atomistic modeling. **Figure 2b** shows how the structure of the hinge region changes when domain 22 is included in SAXS-based elastic network models. Because the structure has not been well established from experiments alone, these authors used REMD to predict the atomistic structure of the exon 21–23 domains (WT+22 hinge) and the 21/23 domains (WT) (**Figure 2c**). The structures obtained from REMD were confirmed by SAXS and showed that inclusion of domain 22 causes a structural transition from more flexible helices to stiffer β-sheets. The authors utilized elastic network models in which proteins are described as a set of beads that are interconnected with elastic springs; such models can be a useful tool to study the relation between structures and dynamics of proteins (69–71). The elastic network model shows that excluding domain 22 changes the dynamics of the hinge part significantly, and its vibrational behavior can critically affect the self-assembly of tropoelastin. This study (68) demonstrated that molecular and coarse-grained simulations could reveal the unknown structures and roles of specific parts of proteins in muscular-skeletal systems.

Although the results of this study indicate that the dynamics of tropoelastin may play a critical role in self-assembly of the molecules, the entire tropoelastin molecule is much larger, and usually many molecules are required in order to observe their aggregations. Atomistic MD cannot handle these complexities; thus, CGMD can be utilized to determine the aggregation mechanisms at the micrometer scale. Although CGMD based on the MARTINI force field, for instance, is able to perform aggregation simulations for short segments (tripeptides) (**Supplemental Figure 5**) (72), the force field needs to be improved for simulations of longer elastin-like peptides (73).

▶ Supplemental Material

3.2. Molecular Dynamics of Collagen

One of the most abundant proteins in the human body is collagen. The collagen molecule is the main component of ligaments, tendons, and bones, giving rise to the muscular-skeletal systems' stability and high elasticity. Although there are various types of collagens, their basic building block is a repeating sequence of the Gly–X–Y triplet, where X and Y are commonly proline and
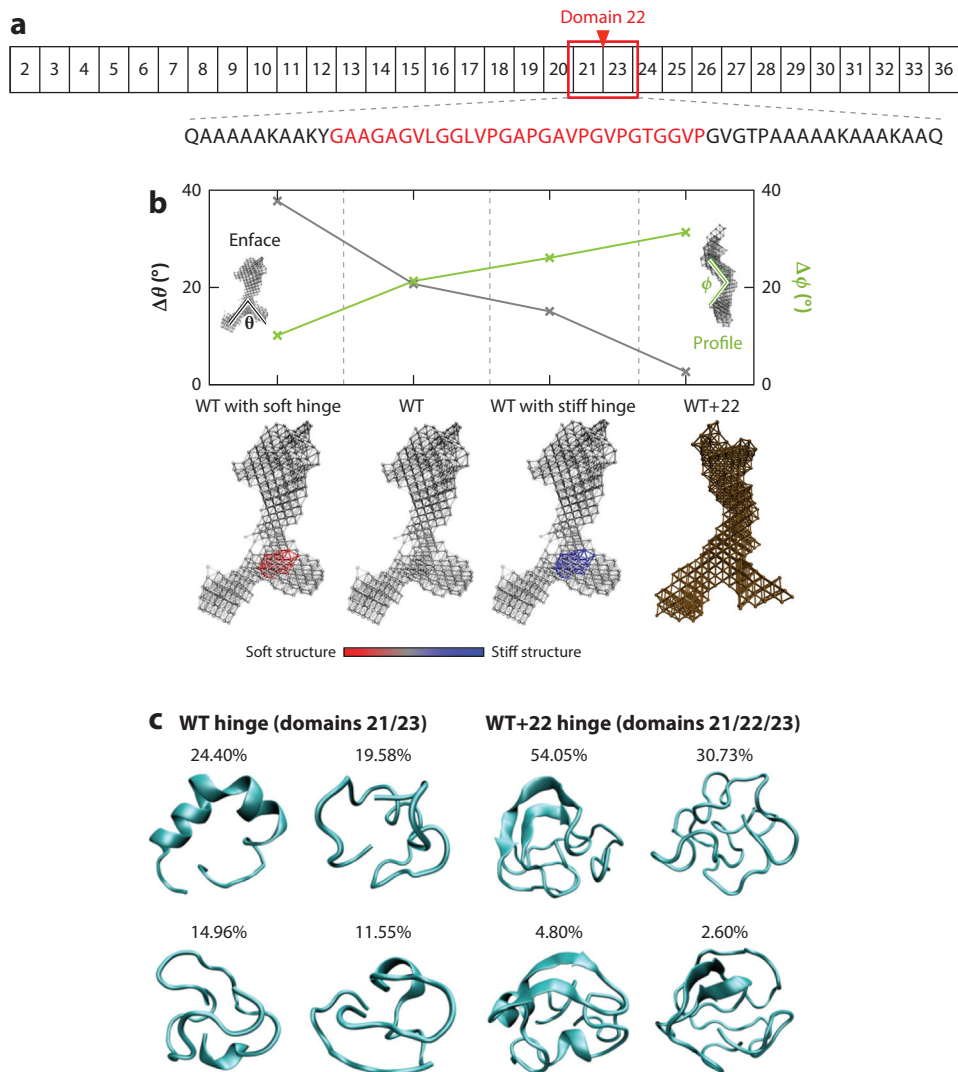
Figure 2

(*a*) Human elastin exons are shown with the specific sequence of domains 21 to 23. The red amino acids represent domain 22. (*b*) Elastic network models of tropoelastin with different stiffnesses of the hinge show structural changes. (*c*) Structures of wild type (WT) and wild type with domain 22 (WT+22) are predicted from replica exchange molecular dynamics. Panels *b* and *c* modified from Reference 68, licensed under CC BY-NC 4.0.

hydroxyproline. The most abundant collagen in the muscular-skeletal systems is fibrillar type I. Three chains of the repeated triplets form a triple-helix structure of tropocollagen molecules. The structure of type I collagen is depicted in **Figure 3a**. In a single unit cell, where the axial length is 67 nm (also known as the D period), five molecular segments are packed into a quasi-hexagonal structure. The unit cell consists of an overlap region (0.46D ∼ 31 nm) and a gap region (0.54D ∼ 36 nm), forming a fibril with a right-handed twist with neighboring fibrils (74).
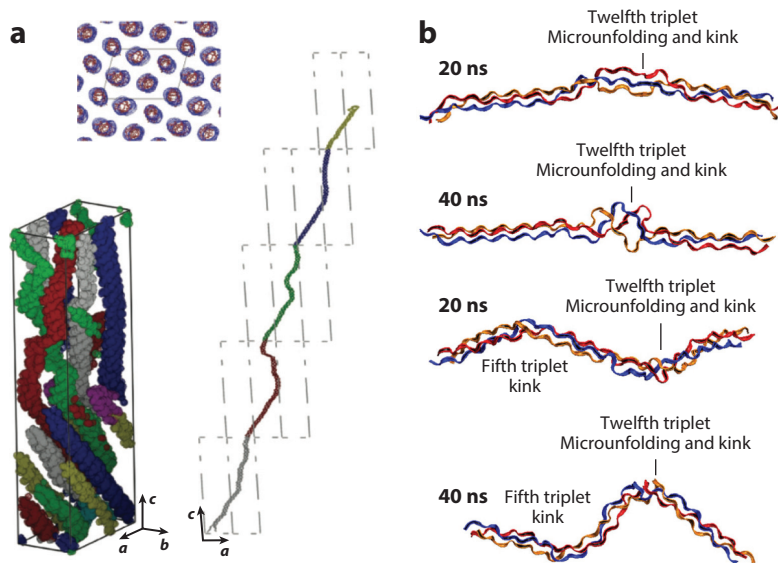
Figure 3

(*a*) The structure of type I collagen shows quasi-hexagonal packing. (*b*) The structures of tropocollagen molecules. (*Top*) Snapshots of heterotrimer (two α-1 chain and one α-2 chain) collagen molecules at 20 ns and 40 ns. (*Bottom*) Snapshots of homotrimer (three α-1 chain) collagen molecules in osteogenesis imperfecta at 20 ns and 40 ns. The homotrimer collagen molecule has larger kinked angles, which may result in greater lateral distances in the microfibril. Panel *a* modified with permission from Reference 74. Copyright 2006, National Academy of Sciences. Panel *b* modified with permission from Reference 77. Copyright 2012, Elsevier.

The mechanical properties and deformation of a single collagen molecule have been well characterized from atomistic simulations. Young's modulus measurements from MD (∼4 GPa) are in excellent agreement with those from experiments (∼3–5 GPa) (75, 76). Also, MD simulation reveals that there is a loading-rate dependency under tensile loading. Because the three chains form a triple helix by H-bonds, deformation under tensile loading involves unwinding of the triple helix followed by breaking of H-bonds. Then, the load bearing transits from the breaking of H-bonds to the stretching of covalent bonds of backbone chains, leading to the hyperelasticity of collagen molecules (75).

Mutations of amino acid in type I collagen are related to genetic disorders such as osteogenesis imperfecta (OI). Atomistic MD has been utilized to reveal the structural and mechanical differences between heterotrimer (WT) and homotrimer (OI) collagen molecules of a mouse model (**Figure 3*b***). Although performing direct aggregations is not possible, MD simulations can show that the mutations distort the structure and cause kinks, which possibly affect the aggregation of collagen fibrils and degrade the mechanical properties of bones and tendons (77). However, MD ceases to be feasible for studies of deformation and failure at the fibril level, so the use of CGMD is required (**Figure 1**).

3.3. Coarse-Grained Molecular Dynamics of Collagen Fibril

Unlike that of elastin, the structure of tropocollagen is well established and stable (74). Thus, it is possible to coarsen the system more than the MARTINI force field does, with a focus on
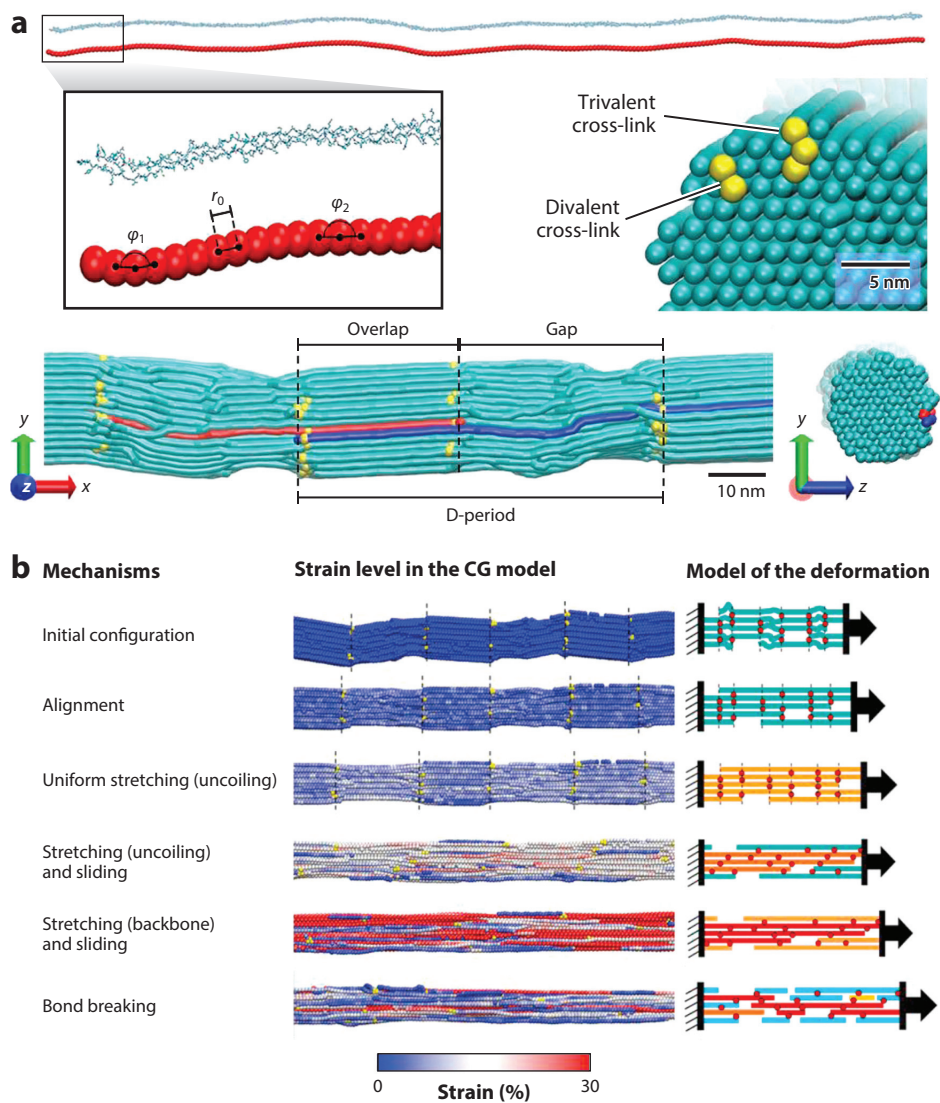
Figure 4

(*a*) The coarse-grained (CG) model of collagen fibrils and cross-links. A single tropocollagen molecule is 300 nm long. The fibril model is composed of 155 CG tropocollagen molecules. (*b*) Deformation of collagen fibrils in the CG model with 50% cross-links demonstrates multiple stages of deformation. Modified with permission from Reference 78. Copyright 2015, Elsevier.

the mechanical properties and deformation of the collagen fibril. Depalle et al. (78) have studied the effects of cross-links on the mechanical properties and deformation of collagen fibrils with their CG model (**Figure 4*a***). The triple-helical tropocollagen molecule is represented by a single chain of beads that have equilibrium distances between them close to the diameter of a tropocollagen molecule. These authors developed the parameters on the basis of a previous model that could capture nonlinear stress–strain behaviors by adopting bilinear spring constants derived from atomistic MD simulations (79, 80). This study utilized a reactive force field (REAX) to

obtain unknown parameters for the cross-links. **Figure 4*b*** shows the deformation of collagen fibril with cross-links. Several regions of deformation enable huge amounts of energy to be dissipated, which cannot be captured with MD simulations of a single collagen molecule. As the density of cross-links increases, the mechanical properties change by activating a second elastic regime that has a different stiffness based on the density of the cross-links.

The effect of mutations on fibril packing is a challenging topic that so far has not been explored with either MD or CGMD due to the limitations of timescale and force fields. Because accurate thermodynamic properties are critical for describing assembly behavior, the MARTINI force field is a likely candidate for self-assembly simulations, as highlighted by tripeptide simulations. The original MARTINI force field does not have parameters for hydroxyproline, an important nonstandard amino acid in collagen molecules; to this end, Gautieri et al. (81) have proposed a parameter set in the MARTINI force field for hydroxyproline from atomistic simulations (**Supplemental Figure 6**). Self-assembly simulations require many units of molecules and may not be possible with the conventional MD/CGMD method due to the problem of multiple local minima. One can approach this issue with enhanced sampling methods such as REMD for the aggregation behavior of segmented type I collagen molecules with CGMD, enabling direct observation of abnormal aggregation due to the mutations. We note that this bottom-up approach of multiscale modeling can be very powerful in understanding the effects of a factor that is difficult to control in vivo and in vitro because it does not require parameters determined a priori from experiments.

Collagen fibrils form collagen fibers that often join together with proteoglycans (PGs) (82), which consist of a core protein and covalently bonded glycosaminoglycan (GAG) chains and are categorized by the size and type of GAGs (83). PGs play an important role as lubricant in cartilage, and GAGs can bridge between contiguous fibrils (84). Although the mechanical roles of collagen fibrils in tendon have been extensively studied, the roles of PGs and GAGs are relatively less well known. Redaelli et al. (85) have performed tensile tests of GAG chains with atomistic MD simulations to obtain stiffness and applied the value to their multifibril model, revealing the importance of collagen fibril length for the elastic properties of tendons. However, previous studies largely failed to explore the failure behaviors at the fiber level, a shortcoming that could be addressed by more systematic investigations with multiscale modeling tools.

4. MULTISCALE MODELING OF MINERAL AND BONE

Bone is arguably the most interesting component of the muscular-skeletal systems because its mechanical properties are extraordinary in terms of both stiffness and toughness, and because of the extraordinary role mineralized tissues like bone have played in evolution. The basic building blocks of bone are collagen and carbonated HAP minerals (7). As shown in the case studies of elastin and collagen, above, the systematic understanding of the properties of bone at a lower hierarchical level is critical for constructing models of the higher level. In this section, we review multiscale modeling of minerals with collagen in bone and emphasize the importance of the quality of minerals in the multiscale modeling of bone.

4.1. Quantum Simulation and Molecular Dynamics of Mineral

The main component of the minerals that can be found in bone is HAP, which is deposited along the collagen fibril direction in the (001) direction (z axis). **Figure 5*a*** shows the structure of HAP [$Ca_5(PO_4)_3(OH)$]. Nanoindentation experiments demonstrate that bulk HAP is a highly anisotropic material in terms of its fracture toughness and Young's modulus (86). Because HAP is the main component of bone, providing stiffness, knowledge of the mechanical
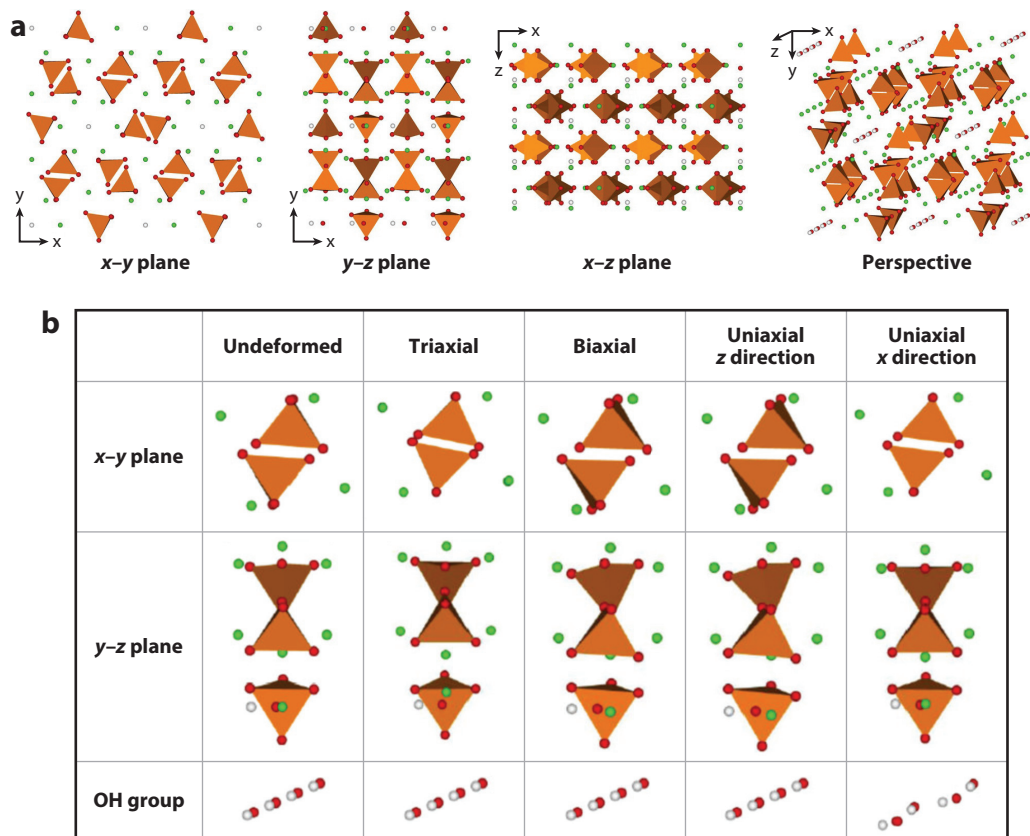
Figure 5

(*a*) The supercell structure of hydroxyapatite in different directions. (*b*) Changes in the local structures at the failure differ under different loading conditions (PO_4, yellow-brown tetrahedral; Ca, green; OH, red/white). Modified from Reference 87 with permission from Macmillan.

properties of pure HAP is important in order to understand their effects on bone. Misra & Ching (87) have studied the mechanical responses of HAP under various loading conditions with DFT. The atomistic deformation of pure HAP under different loadings is difficult to capture from experiments, and DFT calculations help pinpoint the origins of its mechanical properties. Results show path-dependent mechanical responses under multiaxial tensile loading conditions. **Figure 5b** depicts the various changes of the local structures under different loading conditions. This complexity comes from the ionic bonding of HAP, which is not as strong as covalent bonds; therefore, the local structure easily changes (e.g., rotations of PO_4 molecules and distortions of OH molecules) according to the loading path. This path dependency results in the complex nonlinearity and anisotropic behaviors of HAP.

In bone, minerals do not exist as pure HAP because they are substituted by carbonates (CO_3). The carbonate content of bone is ~4–8 wt%. There are two types of carbonate substitutions in HAP: The A type replaces the hydroxyl ions, and the B type replaces the phosphate ions. The B type is significantly more predominant than the A type in bone. Because B-type substitution decreases the crystallinity and increases the solubility of minerals (22), the mechanical properties of minerals in bone can change accordingly.

Each mineral is shaped as a plate with the following approximate dimensions: length, 9 (± 3) nm; width, 6 (± 2) nm; thickness, 2 (± 1.2) nm (88). In particular, lower thickness and poor crystallinity of the mineral plates are important features in OI (89). Using MD simulations, Qin et al. (90) have shown that the binding between collagen and minerals becomes stronger as the mineral thickness increases. Moreover, the mechanical properties of HAP itself significantly degrade under 2 nm (54). The lattice constant of HAP in the thickness direction is ~0.9 nm so that 2 nm is only approximately two unit cells of HAP. Because the stability of HAP comes from ionic interactions, the well-ordered structure is vital for its stability and mechanical properties.

However, the effects of carbonate substitution and crystallinity on the mechanical properties of HAP have been oversimplified in atomistic models. **Figure 6** shows how the crystallinity of HAP correlates with its diffraction patterns and mechanical properties from MD simulations. The X-ray diffraction pattern and selected area diffraction (SAD) pattern are the typical ways to represent the mineralization of collagen fibrils. **Figure 6b** shows a representative SAD pattern of HAP in the (001) direction. **Figure 6c** depicts X-ray powder diffraction patterns of different aged bones, showing that more distinct peaks appear as bones become mature (91, 92). As shown by Olszta et al. (7), the peaks of the diffraction patterns become distinct as the mineralization process occurs, and the broadly diffused diffraction patterns indicate amorphous or poorly crystallized minerals. Some isolated fibrils from mature equine bone do not show distinct diffraction patterns due to natural remodeling and rearrangement, implying that the mineralized collagen fibrils in mature bone can have various crystalline structures.

MD simulations allow us to clarify how mechanical properties can vary due to the quality of the minerals. One can derive the disordered system from pristine HAP by randomly switching two ions. The mechanical properties from the structures thus obtained show that Young's modulus can drastically decrease by more than 60% while the density of the minerals decreases by only 10% due to the degree of crystallinity (**Figure 6d**). These results are in good agreement with experimental observations that mechanical properties and fatigue properties of bone have a significant correlation with the mineral's crystallinity: Crystallinity accounts for 6.7% to 48.3% of the variation in monotonic mechanical properties (93). The effect of crystallinity on the mechanical properties should be considered in higher hierarchical modeling, especially for bone-related diseases such as OI, and skeletal fluorosis caused by excessive accumulation of fluoride in bone (89, 94).

4.2. Molecular Dynamics of Mineralized Collagen Fibril

Building a model with the proper configuration of mineralized collagen fibrils is both relevant and challenging. In an early study (79), researchers proposed a simple two-dimensional (2D) MD model of mineralized collagen fibrils to study their fracture properties. This study described a toughening mechanism at the molecular scale induced by mineralization, which protects the structural integrity of collagen fibrils from catastrophic failure by forming local yield regions that increase energy dissipation. Almora-Barrios & de Leeuw (95) made an early attempt to use atomistic MD to describe the nucleation of mineral phases within the collagen template—from solution. They observed early stages of calcium phosphate clusters near the collagen surface due to charge interactions. However, full mineralization was not observed due to the prohibitive timescale needed in the MD simulation. An alternative method is to adopt a Monte Carlo approach to obtain the structure of mineralized protein matrixes. Nair et al. (96) constructed a mineralized collagen model from a pure collagen molecule in a periodic box by superimposing a HAP unit cell without overlapping on the basis of the distance from the collagen protein phase. The model showed that the tensile modulus increases monotonically as the mineral density increases. One limitation of this model is that it could not account for the specific crystallinity of HAP crystals,
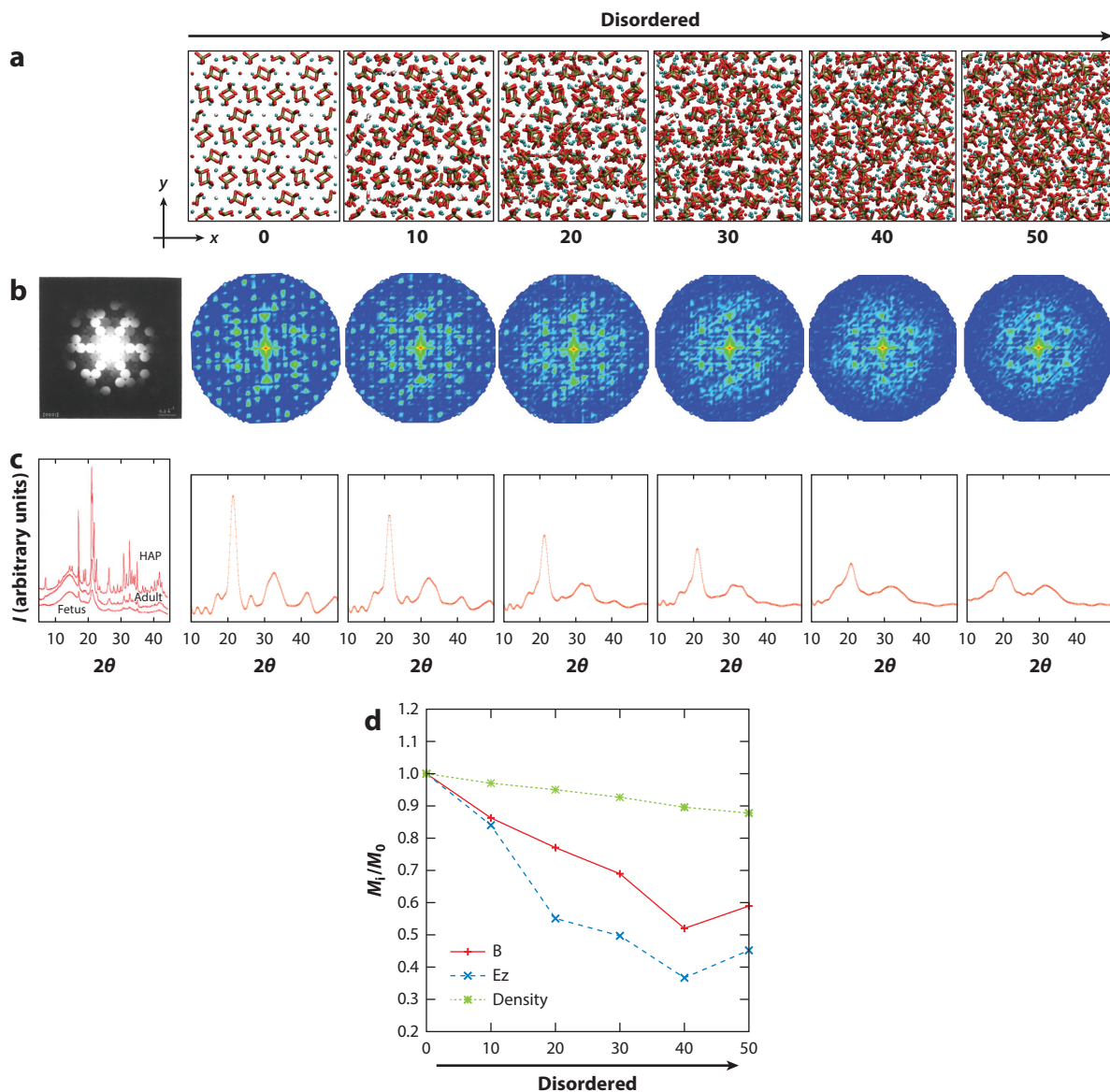
Figure 6

(*a*) Models of different crystallinity generated from pristine hydroxyapatite (HAP) by switching two randomly selected ions. (*b*) Selected area diffraction patterns of HAP (human tooth enamel) in the (001) direction were obtained from an experiment and models (110). (*c*) X-ray diffraction patterns were obtained from fetal and adult bones and models; X-ray powder diffraction patterns were calculated from the debyer program (**https://code.google.com/p/debyer/**). (*d*) The normalized mechanical properties (bulk modulus and Young's modulus on the *z* axis) and densities as a function of the switching number. The numbers indicate how many times the switching process occurs with relaxations. Image of diffraction in panel *b* modified from Reference 111. Image of diffraction in panel *c* reproduced with permission from Reference 112. Copyright 2002, Elsevier.

resulting in oversimplification of the quality of the minerals. By contrast, Duchstein & Zahn (97) proposed a mineral–collagen composite in which the crystal structure of minerals is well preserved. Although their enamel-like composite has a higher mineral density than bone, their approach can be employed to model mineralized collagen fibrils to study the effects of crystallinity. A single unit cell of mineralized collagen can be characterized with MD simulations, but it is not possible to model deformation and failure of fibrils in atomistic simulations.

4.3. Coarse-Grained Molecular Dynamics of Mineralized Collagen Fibril

Recently, Depalle et al. (98) studied the effects of mineral content on the deformation and mechanical properties of mineralized collagen fibrils with CGMD (**Supplemental Figure 7**). Similar to the effects of cross-links in collagen fibrils, as the mineral content increases, the stiffness increases. Above a certain percentage of mineralization (around 30% to 35%), the mineralized collagen behaves more like brittle materials with degraded toughness and density, a behavior that was not captured by MD simulations due to size limitations in the fully atomistic model. Compared with those of nonmineralized collagen fibrils, the strength and toughness of mineralized collagen fibrils can improve by a factor of 10 and 35, respectively.

We note that most modeling of mineralized collagens focuses on the minerals in the gap region of collagen fibrils. However, a study using transmission electron microscope images of cry-ion-milled sections of bones suggests that most ordered minerals are actually deposited in the extrafibrillar space, and that the minerals in the gap zone may not be well crystallized (99, 100). Although the spatial distribution of minerals in bone is still a matter of debate, further studies with multiscale models including information about mineral quality will help uncover the role of intra- and extrafibrillar minerals in bone.

4.4. Continuum Model of Osteon

Few attempts have been made to model fiber patterns or arrays of mineralized collagens with either CGMD or FEM (101). However, the deformation and failure of osteon levels can be modeled with FEM. An important toughening mechanism of osteons is the formation of microcracks rather than the ability to resist crack initiation. Jonvaux et al. (102) have studied microfracture and crack bridging of bone under compression with light microscopy and FEM. They utilized cohesive zone modeling to describe tearing of collagen fibrils with parameters obtained from experiments. The model was built from light microscopy, and the microcrack initiation and deformation behaviors accorded well with experimental observations (**Supplemental Figure 8**). Although the toughness thus obtained under compression was underestimated, this model well described the important roles of microstructures and heterogeneities in deformation and failure of bone. As the input parameters for this model are derived from experiments, the bottom-up approach of multiscale modeling still requires significant effort to connect the micrometer scale to the millimeter scale.

5. BIOINSPIRED HETEROGENEOUS MATERIALS DESIGNS

Each component of the muscular-skeletal systems has a unique structural feature at every hierarchical level, from the nanoscale to the macroscale, and the heterogeneity at each level can play a key role in toughening mechanisms (7, 14). Through computational modeling, a target system can be simplified with a few controllable parameters in order to test their response. Thus, derivation of these parameters at each hierarchical level is fundamental for multiscale modeling. The best way to test and validate a hypothesis from multiscale modeling is to construct a representative

physical structure and check whether its effects correspond with expectations from modeling. This has been a challenging issue, as conventional manufacturing processes that replicate the complex geometries of muscular-skeletal systems are either time consuming or very expensive, or both. Additive manufacturing technology, including 3D printing, is capable of rapidly manufacturing such complex geometries, enabling validations and further material designs based on an improved understanding of these systems (33). Currently, the resolution of 3D printing extends down to 100 nm, allowing the manufacture of materials close to the scale of the basic building blocks of the muscular-skeletal systems (103).

5.1. Designs Inspired by Mineralized Collagen

Dimas et al. (104) have used 3D printing to study mineralized collagen–like composites based on stiff and soft polymer materials (**Supplemental Figure 9**). They have confirmed two main toughening mechanisms of the composite under tensile loadings: (*a*) delocalization of stress concentration due to microcrack formation and (*b*) distinct crack deflection. Models and experiments aided by 3D printing enable the design of bioinspired materials and testing of the specific roles of components such as geometry and ratio of stiffness in order to obtain a deeper understanding of the individual roles of minerals and collagen molecules.

5.2. Designs Inspired by Osteons

Conventional 3D printing materials are very lightweight but weak compared with conventional engineering materials. Researchers have proposed the use of fiber-reinforced polymers to overcome the weakness of these materials (105). However, the resolution of the technique is limited to the millimeter scale, and the fiber orientations are not easily controllable. Martin et al. (106) have proposed a new technology utilizing magnetic nanoparticles (size, ~10 nm) to produce different fiber orientations by varying a magnetic field (resolution, ~10 μm). Although the resolution of the geometry is only ~100 μm, the technology enables production of hierarchical structures from the nanoscale. The tensile strengths of simple osteon-like geometries change with different reinforcement orientations (**Supplemental Figure 10**). The circular reinforcement demonstrates fracture resistance to tensile loading in all directions. This is a promising way to construct more complex bonelike structures and systematically study the effects of hierarchical structures and directions of fibers.

5.3. Hierarchical and Heterogeneous Designs

According to multiscale modeling, each hierarchical part of a muscular-skeletal system can have different scales of heterogeneity (e.g., the content or quality of the mineral in mineralized collagen fibrils, the cross-link density of collagen fibrils, and the shape of osteon) from the nanoscale to the macroscale. Heterogeneities of bone, such as ordered and disordered phases at different length scales, are also observed in experiments (15). However, previous studies using 3D printing focused mainly on repeated geometries at one length scale. Determining the effects of different length scales of heterogeneity on toughening mechanisms can offer promising avenues for characterization and synthesis of the muscular-skeletal systems.

6. CONCLUSIONS AND FUTURE OPPORTUNITIES

This article has provided an overview of multiscale modeling methods as applied to a selection of structurally relevant muscular-skeletal materials. Multiscale modeling is a paradigm that requires a

broad understanding of multidisciplinary fields of study, integrating and interconnecting various methods. We have reviewed basic concepts, applicable scales and properties, limitations, and widely used advanced algorithms.

The case studies discussed in this review have shown how the different methods can be applied to important materials of muscular-skeletal systems (e.g., elastin, collagen, and minerals) at different hierarchies based on the bottom-up approach. For minerals in bone, crystallinity can be important for understanding the origins of heterogeneous mechanical properties of bone at the nanoscale, which was oversimplified in earlier models.

Multiscale modeling provides an integrated perspective on the deformation and failure of the muscular-skeletal systems at different scales, which is a formidable task with conventional modeling. In particular, it provides insights into the structural and mechanical relations between smaller and larger scales. The effects of mineral content on the mechanical properties and deformation of mineralized collagen are not simple to test either in vivo or in vitro. However, the bottom-up approach of multiscale modeling helps us understand the muscular-skeletal systems even without mechanical data on minerals or collagens from experiments. Although it is relatively challenging to develop continuum models from particle-based models, multiscale modeling will be an essential tool for uncovering hitherto unexplored mechanisms or properties of the muscular-skeletal systems.

Efforts to understand these systems by use of multiscale modeling can contribute to designing novel materials that are simultaneously light, stiff, and tough. The design of complex hierarchical microstructures from the nanoscale to the macroscale has been achieved with 3D printing technology. This technology can help us examine or validate the mechanisms identified through multiscale modeling of the muscular-skeletal systems with precisely designed specimens. Integrating 3D printing and multiscale modeling is a promising way to better understand the muscular-skeletal systems and develop materials comparable to bone and muscle for applications as biomaterials.

DISCLOSURE STATEMENT

The authors are not aware of any affiliations, memberships, funding, or financial holdings that might be perceived as affecting the objectivity of this review.

ACKNOWLEDGMENTS

LITERATURE CITED

1. Arnould-Taylor W. 1998. *A Textbook of Anatomy and Physiology*. Cheltenham, UK: Stanley Thornes
2. Taga G. 1995. A model of the neuro-musculo-skeletal system for human locomotion. *Biol. Cybern.* 73:97–111
3. Frank CB. 2004. Ligament structure, physiology and function. *J. Musculoskelet. Neuronal Interact.* 4:199–201
4. Kannus P. 2000. Structure of the tendon connective tissue. *Scand. J. Med. Sci. Sports* 10:312–20
5. Fox AJS, Bedi A, Rodeo SA. 2009. The basic science of articular cartilage: structure, composition, and function. *Sports Health* 1:461–68

6. Clarke B. 2008. Normal bone anatomy and physiology. *Clin. J. Am. Soc. Nephrol.* 3:S131–39

7. Olszta MJ, Cheng X, Jee SS, Kumar R, Kim Y-Y, et al. 2007. Bone structure and formation: a new perspective. *Mater. Sci. Eng. Rep.* 58:77–116

8. Launey ME, Buehler MJ, Ritchie RO. 2010. On the mechanistic origins of toughness in bone. *Annu. Rev. Mater. Res.* 40:25–53

9. Cassidy JJ, Hiltner A, Baer E. 1989. Hierarchical structure of the intervertebral disc. *Connect. Tissue Res.* 23:75–88

10. Screen HRC, Lee DA, Bader DL, Shelton JC. 2004. An investigation into the effects of the hierarchical structure of tendon fascicles on micromechanical properties. *Proc. Inst. Mech. Eng. H* 218:109–19

11. Keaveny TM, Hayes WC. 1993. A 20-year perspective on the mechanical properties of trabecular bone. *J. Biomech. Eng.* 115:534–42

12. Danielsen CC, Andreassen TT. 1988. Mechanical properties of rat tail tendon in relation to proximal–distal sampling position and age. *J. Biomech.* 21:207–12

13. Escoffier C, de Rigal J, Rochefort A, Vasselet R, Lévêque J-L, Agache PG. 1989. Age-related mechanical properties of human skin: an in vivo study. *J. Investig. Dermatol.* 93:353–57

14. Reznikov N, Shahar R, Weiner S. 2014. Three-dimensional structure of human lamellar bone: the presence of two different materials and new insights into the hierarchical organization. *Bone* 59:93–104

15. Reznikov N, Shahar R, Weiner S. 2014. Bone hierarchical structure in three dimensions. *Acta Biomater.* 10:3815–26

16. Meyers MA, Chen P-Y, Lin AY-M, Seki Y. 2008. Biological materials: structure and mechanical properties. *Prog. Mater. Sci.* 53:1–206

17. Giesa T, Pugno NM, Wong JY, Kaplan DL, Buehler MJ. 2014. What's inside the box? Length scales that govern fracture processes of polymer fibers. *Adv. Mater.* 26:412–17

18. Gao H, Ji B, Jäger IL, Arzt E, Fratzl P. 2003. Materials become insensitive to flaws at nanoscale: lessons from nature. *PNAS* 100:5597–600

19. Kielty CM, Sherratt MJ, Shuttleworth CA. 2002. Elastic fibres. *J. Cell Sci.* 115:2817–28

20. Fratzl P, Weinkamer R. 2007. Nature's hierarchical materials. *Prog. Mater. Sci.* 52:1263–334

21. Fratzl P. 2008. Collagen: structure and mechanics. An introduction. In *Collagen: Structure and Mechanics*, ed. P Fratzl, 1–13. Boston: Springer

22. Landi E, Celotti G, Logroscino G, Tampieri A. 2003. Carbonated hydroxyapatite as bone substitute. *J. Eur. Ceram. Soc.* 23:2931–37

23. Rey C, Collins B, Goehl T, Dickson IR, Glimcher MJ. 1989. The carbonate environment in bone mineral: a resolution-enhanced Fourier transform infrared spectroscopy study. *Calcif. Tissue Int.* 45:157–64

24. Buehler M, Keten S. 2010. Colloquium: failure of molecules, bones, and the Earth itself. *Rev. Mod. Phys.* 82:1459–87

25. Keylock CJ, Constantinescu G, Hardy RJ. 2012. The application of computational fluid dynamics to natural river channels: eddy resolving versus mean flow approaches. *Geomorphology* 179:1–20

26. Monaghan JJ. 2005. Smoothed particle hydrodynamics. *Rep. Prog. Phys.* 68:1703

27. Matsumoto M, Saito S, Ohmine I. 2002. Molecular dynamics simulation of the ice nucleation and growth process leading to water freezing. *Nature* 416:409–13

28. Senftle TP, Hong S, Islam MM, Kylasa SB, Zheng Y, et al. 2016. The ReaxFF reactive-force field: development, applications and future directions. *NPJ Comput. Mater.* 2:15011

29. Ng M-F, Zhou L, Yang S-W, Sim LY, Tan VBC, Wu P. 2007. Theoretical investigation of silicon nanowires: methodology, geometry, surface modification, and electrical conductivity using a multiscale approach. *Phys. Rev. B* 76:155435

30. Hafner J, Wolverton C, Ceder G. 2006. Toward computational materials design: the impact of density functional theory on materials research. *MRS Bull.* 31:659–68

31. Hamed E, Lee Y, Jasiuk I. 2010. Multiscale modeling of elastic properties of cortical bone. *Acta Mech.* 213:131–54

32. Zeng QH, Yu AB, Lu GQ. 2008. Multiscale modeling and simulation of polymer nanocomposites. *Prog. Polym. Sci.* 33:191–269

33. Xiang Gu G, Su I, Sharma S, Voros JL, Qin Z, Buehler MJ. 2016. Three-dimensional printing of bio-inspired composites. *J. Biomech. Eng.* 138:021006–16

34. Murphy SV, Atala A. 2014. 3D bioprinting of tissues and organs. *Nat. Biotechnol.* 32:773–85

35. Libonati F, Gu GX, Qin Z, Vergani L, Buehler MJ. 2016. Bone-inspired materials by design: toughness amplification observed using 3D printing and testing. *Adv. Eng. Mater.* 18:1354–63

36. Sugita Y, Okamoto Y. 1999. Replica-exchange molecular dynamics method for protein folding. *Chem. Phys. Lett.* 314:141–51

37. Georgescu IM, Ashhab S, Nori F. 2014. Quantum simulation. *Rev. Mod. Phys.* 86:153–85

38. Hohenberg P, Kohn W. 1964. Inhomogeneous electron gas. *Phys. Rev. B* 136:864–71

39. Kohn W, Sham LJ. 1965. Self-consistent equations including exchange and correlation effects. *Phys. Rev. A* 140:1133–38

40. Perdew JP, Burke K, Ernzerhof M. 1996. Generalized gradient approximation made simple. *Phys. Rev. Lett.* 77:3865–68

41. Szabó A, Ostlund NS. 1996. *Modern Quantum Chemistry: Introduction to Advanced Electronic Structure Theory*. Mineola, NY: Dover

42. van der Kamp MW, Shaw KE, Woods CJ, Mulholland AJ. 2008. Biomolecular simulation and modelling: status, progress and prospects. *J. R. Soc. Interface* 5:S173–90

43. Alder BJ, Wainwright TE. 1959. Studies in molecular dynamics. I. General method. *J. Chem. Phys.* 31:459–66

44. Rahman A. 1964. Correlations in the motion of atoms in liquid argon. *Phys. Rev. A* 136:405–11

45. MacKerell AD Jr., Bashford D, Bellott M, Dunbrack RL Jr., Evanseck JD, et al. 1998. All-atom empirical potential for molecular modeling and dynamics studies of proteins. *J. Phys. Chem. B* 102:3586–616

46. Cornell WD, Cieplak P, Bayly CI, Gould IR, Merz KM, et al. 1995. A second generation force field for the simulation of proteins, nucleic acids, and organic molecules. *J. Am. Chem. Soc.* 117:5179–97

47. Christen M, Hünenberger PH, Bakowies D, Baron R, Bürgi R, et al. 2005. The GROMOS software for biomolecular simulation: GROMOS05. *J. Comput. Chem.* 26:1719–51

48. Lindorff-Larsen K, Maragakis P, Piana S, Eastwood MP, Dror RO, et al. 2012. Systematic validation of protein force fields against experimental data. *PLOS ONE* 7:e32131

49. Verlet L. 1967. Computer "experiments" on classical fluids. I. Thermodynamical properties of Lennard-Jones molecules. *Phys. Rev.* 159:98–103

50. Nosé S. 1984. A unified formulation of the constant temperature molecular dynamics methods. *J. Chem. Phys.* 81:511–10

51. Hoover WG. 1985. Canonical dynamics: equilibrium phase-space distributions. *Phys. Rev. A* 31:1695–97

52. Martyna GJ, Klein ML, Tuckerman M. 1992. Nosé–Hoover chains: the canonical ensemble via continuous dynamics. *J. Chem. Phys.* 97:2635–10

53. Andersen HC. 1983. Rattle: a "velocity" version of the shake algorithm for molecular dynamics calculations. *J. Comput. Phys.* 52:24–34

54. Jung GS, Qin Z, Buehler MJ. 2015. Mechanical properties and failure of biopolymers: atomistic reactions to macroscale response. *Top. Curr. Chem.* 369:317–43

55. Buehler MJ. 2007. Hierarchical chemo-nanomechanics of proteins: entropic elasticity, protein unfolding and molecular fracture. *J. Mech. Mater. Struct.* 2:1019–57

56. van Duin ACT, Dasgupta S, Lorant F, Goddard WA. 2001. ReaxFF: a reactive force field for hydrocarbons. *J. Phys. Chem. A* 105:9396–409

57. Buehler MJ, van Duin ACT, Goddard WA. 2006. Multiparadigm modeling of dynamical crack propagation in silicon using a reactive force field. *Phys. Rev. Lett.* 96:095505

58. Marrink SJ, Risselada HJ, Yefimov S, Tieleman DP, de Vries AH. 2007. The MARTINI force field: coarse grained model for biomolecular simulations. *J. Phys. Chem. B* 111:7812–24

59. Marrink SJ, Tieleman DP. 2013. Perspective on the MARTINI model. *Chem. Soc. Rev.* 42:6801–22

60. Griffith AA. 1921. The phenomena of rupture and flow in solids. *Philos. Trans. R. Soc. A* 221:163–98

61. Irwin GR. 1957. Analysis of stresses and strains near the end of a crack traversing a plate. *J. Appl. Mech.* 24:361–64

62. Jung GS, Qin Z, Buehler MJ. 2015. Molecular mechanics of polycrystalline graphene with enhanced fracture toughness. *Extreme Mech. Lett.* 2:52–59

63. Plimpton S. 1995. Fast parallel algorithms for short-range molecular dynamics. *J. Comput. Phys.* 117:1–19

64. Bowers KJ, Dror RO, Shaw DE. 2006. The midpoint method for parallelization of particle simulations. *J. Chem. Phys.* 124:184109
65. Kessel A, Ben-Tal N. 2011. *Introduction to Proteins: Structure, Function, and Motion*. Boca Raton, FL: CRC
66. He D, Miao M, Sitarz EE, Muiznieks LD, Reichheld S, et al. 2012. Polymorphisms in the human tropoelastin gene modify in vitro self-assembly and mechanical properties of elastin-like polypeptides. *PLOS ONE* 7:e46130
67. Miao M, Cirulis JT, Lee S, Keeley FW. 2005. Structural determinants of cross-linking and hydrophobic domains for self-assembly of elastin-like polypeptides. *Biochemistry* 44:14367–75
68. Yeo GC, Tarakanova A, Baldock C, Wise SG, Buehler MJ, Weiss AS. 2016. Subtle balance of tropoelastin molecular shape and flexibility regulates dynamics and hierarchical assembly. *Sci. Adv.* 2:e1501145
69. Tirion MM. 1996. Large amplitude elastic motions in proteins from a single-parameter, atomic analysis. *Phys. Rev. Lett.* 77:1905–8
70. Hinsen K. 1998. Analysis of domain motions by approximate normal mode calculations. *Proteins Struct. Funct. Bioinform.* 33:417–29
71. Bahar I, Rader AJ. 2005. Coarse-grained normal mode analysis in structural biology. *Curr. Opin. Struct. Biol.* 15:586–92
72. Frederix PWJM, Scott GG, Abul-Haija YM, Kalafatovic D, Pappas CG, et al. Exploring the sequence space for (tri-)peptide self-assembly to design and discover new hydrogels. *Nat. Chem.* 7:30–37
73. Seo M, Rauscher S, Pomès R, Tieleman DP. 2012. Improving internal peptide dynamics in the coarse-grained MARTINI model: toward large-scale simulations of amyloid- and elastin-like peptides. *J. Chem. Theory Comput.* 8:1774–85
74. Orgel JPRO, Irving TC, Miller A, Wess TJ. 2006. Microfibrillar structure of type I collagen in situ. *PNAS* 103:9001–5
75. Gautieri A, Buehler MJ, Redaelli A. 2009. Deformation rate controls elasticity and unfolding pathway of single tropocollagen molecules. *J. Mech. Behav. Biomed. Mater.* 2:130–37
76. Sasaki N, Odajima S. 1996. Stress–strain curve and Young's modulus of a collagen molecule as determined by the X-ray diffraction technique. *J. Biomech.* 29:655–58
77. Chang S-W, Shefelbine SJ, Buehler MJ. 2012. Structural and mechanical differences between collagen homo- and heterotrimers: relevance for the molecular origin of brittle bone disease. *Biophys. J.* 102:640–48
78. Depalle B, Qin Z, Shefelbine SJ, Buehler MJ. 2015. Influence of cross-link structure, density and mechanical properties in the mesoscale deformation mechanisms of collagen fibrils. *J. Mech. Behav. Biomed. Mater.* 52:1–13
79. Buehler MJ. 2007. Molecular nanomechanics of nascent bone: fibrillar toughening by mineralization. *Nanotechnology* 18:295102
80. Buehler MJ. 2006. Nature designs tough collagen: explaining the nanostructure of collagen fibrils. *PNAS* 103:12285–90
81. Gautieri A, Russo A, Vesentini S, Redaelli A, Buehler MJ. 2010. Coarse-grained model of collagen molecules using an extended MARTINI force field. *J. Chem. Theory Comput.* 6:1210–18
82. Birk DE, Zycband E. 1994. Assembly of the tendon extracellular matrix during development. *J. Anat.* 184:457–63
83. Iozzo RV, Schaefer L. 2015. Proteoglycan form and function: a comprehensive nomenclature of proteoglycans. *Matrix Biol.* 42:11–55
84. Knudson CB, Knudson W. 2001. Cartilage proteoglycans. *Semin. Cell Dev. Biol.* 12:69–78
85. Redaelli A, Vesentini S, Soncini M, Vena P, Mantero S, Montevecchi FM. 2003. Possible role of decorin glycosaminoglycans in fibril to fibril force transfer in relative mature tendons—a computational study from molecular to microstructural level. *J. Biomech.* 36:1555–69
86. Viswanath B, Raghavan R, Ramamurty U, Ravishankar N. 2007. Mechanical properties and anisotropy in hydroxyapatite single crystals. *Scr. Mater.* 57:361–64
87. Misra A, Ching WY. 2013. Theoretical nonlinear response of complex single crystal under multi-axial tensile loading. *Sci. Rep.* 3:1488
88. Kuhn L, Eppell SJ, Tong W, Glimcher MJ, Katz JL. 2003. Size and shape of mineralites in young bovine bone measured by atomic force microscopy. *Calcif. Tissue Int.* 72:592–98

89. Fratzl P, Paris O, Klaushofer K, Landis WJ. 1996. Bone mineralization in an osteogenesis imperfecta mouse model studied by small-angle X-ray scattering. *J. Clin. Investig.* 97:396–402

90. Qin Z, Gautieri A, Nair AK, Inbar H, Buehler MJ. 2012. Thickness of hydroxyapatite nanocrystal controls mechanical properties of the collagen–hydroxyapatite interface. *Langmuir* 28:1982–92

91. Meneghini C, Dalconi MC, Nuzzo S, Mobilio S, Wenk RH. 2003. Rietveld refinement on X-ray diffraction patterns of bioapatite in human fetal bones. *Biophys. J.* 84:2021–29

92. Pastenes ES, Reyes-Gasga J. 2001. Computer simulation of selected and convergent beam electron diffraction patterns for hydroxyapatite. *Rev. Latinoam. Metal. Mater.* 21:69–73

93. Yerramshetty JS, Akkus O. 2008. The associations between mineral crystallinity and the mechanical properties of human cortical bone. *Bone* 42:476–82

94. Farlay D, Panczer G, Rey C, Delmas P, Boivin G. 2010. Mineral maturity and crystallinity index are distinct characteristics of bone mineral. *J. Bone Miner. Metab.* 28:433–45

95. Almora-Barrios N, de Leeuw NH. 2010. Modelling the interaction of a Hyp-Pro-Gly peptide with hydroxyapatite surfaces in aqueous environment. *CrystEngComm* 12:960–67

96. Nair AK, Gautieri A, Chang S-W, Buehler MJ. 2013. Molecular mechanics of mineralized collagen fibrils in bone. *Nat. Commun.* 4:1724

97. Duchstein P, Zahn D. 2010. Atomistic modeling of apatite–collagen composites from molecular dynamics simulations extended to hyperspace. *J. Mol. Model.* 17:73–79

98. Depalle B, Qin Z, Shefelbine SJ, Buehler MJ. 2016. Large deformation mechanisms, plasticity, and failure of an individual collagen fibril with different mineral content. *J. Bone Miner. Res.* 31:380–90

99. Schwarcz HP. 2015. The ultrastructure of bone as revealed in electron microscopy of ion-milled sections. *Semin. Cell Dev. Biol.* 46:44–50

100. Schwarcz HP, McNally EA, Botton GA. 2014. Dark-field transmission electron microscopy of cortical bone reveals details of extrafibrillar crystals. *J. Struct. Biol.* 188:240–48

101. Reisinger AG, Pahr DH, Zysset PK. 2010. Sensitivity analysis and parametric study of elastic properties of an unidirectional mineralized bone fibril array using mean field methods. *Biomech. Model. Mechanobiol.* 9:499–510

102. Jonvaux J, Hoc T, Budyn É. 2012. Analysis of micro fracture in human Haversian cortical bone under compression. *Int. J. Numer. Methods Biomed. Eng.* 28:974–98

103. Patel P. 2013. Micro 3-D printer creates tiny structures in seconds. *MIT Technology Review*, March 5. **https://www.technologyreview.com/s/511856/micro-3-d-printer-creates-tiny-structures-in-seconds/**

104. Dimas LS, Bratzel GH, Eylon I, Buehler MJ. 2013. Tough composites inspired by mineralized natural materials: computation, 3D printing, and testing. *Adv. Funct. Mater.* 23:4629–38

105. Grunenfelder LK, Suksangpanya N, Salinas C, Milliron G, Yaraghi N, et al. 2014. Bio-inspired impact-resistant composites. *Acta Biomater.* 10:3997–4008

106. Martin JJ, Fiore BE, Erb RM. Designing bioinspired composite reinforcement architectures via 3D magnetic printing. *Nat. Commun.* 6:8641

107. Józsa L, Kannus P. 1997. Histopathological findings in spontaneous tendon ruptures. *Scand. J. Med. Sci. Sports* 7:113–18

108. Boundless. 2016. Connective tissue is found throughout the body, providing support and shock absorption for tissues and bones. *Boundless Biology*, May 26. **https://www.boundless.com/biology/textbooks/boundless-biology-textbook/the-animal-body-basic-form-and-function-33/animal-primary-tissues-193/connective-tissues-loose-fibrous-and-cartilage-738-11968/**

109. Phillips ATM, Villette CC, Modenese L. 2015. Femoral bone mesoscale structural architecture prediction using musculoskeletal and finite element modelling. *Int. Biomech.* 2:43–61

110. Coleman SP, Spearot DE, Capolungo L. 2013. Virtual diffraction analysis of Ni [010] symmetric tilt grain boundaries. *Model. Simul. Mater. Sci. Eng.* 21:055020

111. Bres EF, Cherns D, Vincent R, Morniroli JP. 1993. Space-group determination of human tooth-enamel crystals. *Acta Crystallogr. B* 49:56–62

112. Dalconi MC, Meneghini C, Nuzzo S, Wenk R, Mobilio S. 2003. Structure of bioapatite in human foetal bones: an X-ray diffraction study. *Nucl. Instrum. Methods B* 200:406–10